Ligand-mediated contaminant degradation by bare and carboxymethyl cellulose-coated bimetallic palladium-zero valent iron nanoparticles in high salinity environments

Xiaoming Ma[1,2], Di He[1,2,*], Adele M. Jones[3], T. David Waite[3], Taicheng An[1,2]

1. *Institute of Environmental Health and Pollution Control, Guangdong University of Technology, Guangzhou 510006, China*
2. *Guangzhou Key Laboratory of Environmental Catalysis and Pollution Control, School of Environmental Science and Engineering, Guangzhou University of Technology, Guangzhou 510006, China*
3. *School of Civil and Environmental Engineering, University of New South Wales, Sydney, NSW 2052, Australia*

ARTICLE INFO

ABSTRACT

The application of nanoscale zero-valent iron (nZVI) for the degradation of contaminants has been extensively investigated, however, few studies have focused on degradation in high salinity environments. In this study, the ability of bare and carboxymethyl cellulose (CMC)-coated bimetallic Pd-nZVI particles to degrade 33′44′-tetrachlorobiphenyl in high saline water (SW) is examined with particular attention given to the effects of ethylenediaminetetraacetic acid (EDTA) on the rate of degradation. EDTA enhances the reactivity of Pd-nZVI in SW, with evidence provided to link this to the removal of the passivating layer. Additionally, a conceptual model is proposed which provides a quantitative description of the removal of these iron oxide layers in the presence of EDTA. An optimum EDTA to bare Pd-nZVI molar ratio of 0.1 exists, with insufficient EDTA unable to remove the passivating layer whilst excess EDTA results in Fe loss and enhanced agglomeration due to magnetic attraction of the bare Fe(0) particles. In contrast, CMC-coating of Pd-nZVI assemblages actually impedes degradation, despite the coated particles displaying a smaller average size compared to uncoated particles, with even the presence of EDTA in this case not significantly improving degradation. The reduced reactivity in the presence of CMC is primarily attributed to the effect of CMC on the association of Pd with nZVI particles. In particular, the presence of CMC reduced the total amount of Pd incorporated with the stabilized particles compared to the non-stabilized particles. Additionally, the presence of CMC results in less Pd present in its reactive zero-valent oxidation state.

© 2018 The Research Center for Eco-Environmental Sciences, Chinese Academy of Sciences. Published by Elsevier B.V.

---

* *Corresponding author.*
  E-mail: di.he@gdut.edu.cn. (D. He).

Introduction

Environmental contamination due to harmful organic pollutants from industrial activities is a significant problem worldwide (WHO, 2010). These organic pollutants are often extremely toxic and highly recalcitrant and, due to their chemical nature, tend to accumulate in fish tissue and the food chain in and can pollute waterways and drinking water supplies (WHO, 2010). As such, there is a dire need to remediate sites contaminated with organic pollutants such as polychlorinated biphenyls (PCBs), the focus of this particular study. PCBs were previously employed as electrical coolants but have since been banned due to their carcinogenicity (Mayes et al., 1998; Mikszewski, 2004). Particular PCB mixtures have been shown to be more toxic than others (Mayes et al., 1998), and, among the PCB congeners, the highly toxic co-planar PCB, 33′44′-tetrachlorobiphenyl (also known as PCB-77), is considered particularly toxic and has therefore been assigned a high priority for research in nZVI remediation studies (Bergen et al., 1996; Danis et al., 2004; Lowry and Johnson, 2004; Mikszewski, 2004).

Traditional techniques for sediment remediation employ *ex situ* treatment, such as dredging, incineration and land filling. These methods, in addition to being highly disturbing to the surrounding environment, may yield even more toxic by-products compared to the initial target contaminants. Furthermore, the cost and the intensive energy consumptions of these techniques are generally considered to outweigh those of *in situ* remediation technologies such as the use of nZVI (Geiger et al., 2009; Grieger et al., 2010; Coutts et al., 2011). As such, there is intense interest in the application of *in situ* remediation techniques. Particular interest has been shown in the use of nanoscale zero-valent iron (nZVI) – a highly effective and environmentally benign nanomaterial which has been shown to immobilize and/or degrade various contaminants including heavy metals (e.g. chromium, arsenic and uranium) (Ponder et al., 2000; Ramos et al., 2009; Xie and Cwiertny, 2010; Yan et al., 2010a; Liang et al., 2014), inorganic contaminants (nitrate and nitrite) (Yang and Lee, 2005; Liou et al., 2006) and organic contaminants such as chlorinated ethanes and polychlorinated biphenyls (PCBs) (Lowry and Johnson, 2004; Liu and Lowry, 2006; Song and Carraway, 2006; Wei et al., 2006). The use of nZVI has already been trialed in a variety of full-scale remediation projects with general consensus that the approach is effective (Elliott and Zhang, 2001; US EPA, 2008; Wei et al., 2010).

Despite the advantages of nZVI technology, concerns have been raised in relation to the efficacy and longevity of this remediation approach (Li et al., 2006; Yan et al., 2010b; O'Carroll et al., 2013). To overcome the above issues, a number of modifications have been successfully applied, such as (1) doping a secondary transition metal to improve the reactivity of nZVI and (2) the application of capping agents to enhance the nZVI stability (Wang and Zhang, 1997; Xu and Bhattacharyya, 2006; He and Zhao, 2008; Sakulchaicharoen et al., 2010). The doped metal (typically Pd, Pt, Ni or Cu) is capable of catalyzing the conversion of H_2 gas that is produced via the interaction of Fe(0) with H_2O, to atomic hydrogen which is regarded as a much stronger

reductants, and therefore dechlorinating agent, compared to Fe(0) (Wang and Zhang, 1997; Zhang et al., 1998; Schrick et al., 2002; Tee et al., 2005; Lien and Zhang, 2007; Shih et al., 2009). A 2 to 3 order of magnitude increase in the reactivity of Pd-nZVI can be achieved relative to the undoped nZVI particles (Wang and Zhang, 1997), whilst a 1 to 2 order of magnitude increase in reactivity has been reported when nZVI particles are doped with Ni (Schrick et al., 2002). Apart from significant acceleration of pollutant degradation, the application of bimetallic particles can also generate by-products which are more extensively dechlorinated and less toxic (Lien and Zhang, 2001; Schrick et al., 2002). Due to van der Waals forces of attractive and magnetic interactions, bare nZVI also suffers from aggregation with the formation large particles or aggregates in a short period of time leading to a decrease in its specific surface area and a subsequent decline in its reaction efficiency (Xie et al., 2014). To prevent the agglomeration of nZVI, particle stabilization is generally achieved using "green" biopolymers such as carboxymethyl cellulose (CMC), chitosan and polyvinylpyrrolidone (PVP), to induce electrostatic and steric repulsion between individual nZVI particles (He and Zhao, 2007; Xie et al., 2016). Other techniques used to prevent the aggregation of magnetic particles could also be of benefit such as the use of metal–organic frameworks to alter the surface charge and therefore enhance electrostatic repulsion between particles (Alqadami et al., 2017, 2018).

While the high reactivity of nZVI particles compared to larger micron-sized ZVI particles is an initial advantage, a passivating layer consisting of, predominantly, Fe(III) oxy (hydr)oxides (termed Fe oxides herein) readily forms on nanosized particles through the reaction of nZVI with non-target substances such as dissolved oxygen, water and/or other solutes in solution. This oxide layer lowers the reducing capacity of nZVI particles by impeding electron transfer from nZVI to the target contaminant/s and/or by reducing the accessibility of the contaminant/s to the doped metal catalyst (Zhu and Lim, 2007). Several methods have been found to be effective at removing these oxide layers including the use of reducing agents (Zhu and Lim, 2007; Xie and Cwiertny, 2010), acid washing, weak magnetic field (Liang et al., 2014; Sun et al., 2014; Qin et al., 2017) and chelating agents such as ethylenediaminetetraacetic acid (EDTA) (Zhu and Lim, 2007; Zhang et al., 2011). All of these substances remove the passivating layer by inducing dissolution of the Fe oxide coating. To date, however, there have been no detailed investigations on the effect of stabilizers on these depassivation strategies, whereby the presence of the stabilizer may affect ligand-assisted dissolution of the Fe oxide coating.

Whilst a number of studies have focused on optimizing the performance of bimetallic nZVI particles, their behaviors in high salinity environments, akin to the harbor or estuarine environments in which PCB contaminated sediments are often found (Ghosh et al., 2003), have only been investigated in a few studies with contradictory conclusions reported. Some studies found that the high ionic strength led to the aggregation of nZVI with inhibition of ZVI corrosion (Reinsch et al., 2010; Xin et al., 2016) while, in other works, chloride and bromide were reported to serve as pitting and crevice corrosion promoters, the presence of which are able to

remove the passivating oxide layer and maintain the degradation efficiency of Fe(0) (Kim et al., 2007; Yin et al., 2012). A recent study by our research group has indicated that the presence of Ca^{2+} and Mg^{2+} promotes the moderate removal of Fe oxide passivation layers via the slow release of EDTA following the dissociation of Ca and Mg-EDTA complexes, improving the effectiveness of EDTA-mediated nZVI depassivation (He et al., 2016). Given the lack of consistent information on the behavior of nZVI particles and the effectiveness of ligand-promoted depassivation of nZVI particles in high salinity environments, the objectives of this study are to quantify and interpret the effects of EDTA on the ability of bare and carboxymethyl cellulose (CMC)-coated Pd-nZVI particles to degrade PCB in a saline matrix. To aid in elucidating its effect a kinetic model of the ligand-promoted mechanism will also be developed.

1. Materials and methods

1.1. Materials

Carboxymethyl cellulose (CMC, MW = 90,000 g/mol), ethylenediaminetetraacetic acid (EDTA), ferrous chloride tetrahydrate ($FeCl_2 \cdot 4H_2O$), sodium borohydride ($NaBH_4$), palladium acetate (reagent grade, 98%), hexane and acetone were purchased from Sigma Aldrich (St. Louis, MO, USA). The polychlorinated biphenyl (100% 33′44′-tetrachlorobiphenyl) and NaOH were obtained from AccuStandard (New Haven, CT, USA) and Chem-Supply (Gillman, SA, Australia), respectively. All aqueous solutions were prepared using 18 MΩ·cm Milli-Q water and stored in the refrigerator at 4°C under dark environments when not in use. Natural saline water (i.e. seawater) was obtained from the Sydney Offshore Reference Station and filtered before use through 0.22 μm Durapore PVDF filters, while synthetic freshwater (FW) was prepared using 2 mmol/L $NaHCO_3$ with minor adjustment of pH to 8.3, which was similar to that of the collected natural seawater. All solutions were de-aerated by purging with high purity (99.997%) argon gas for at least 2 hr before use with all experiments undertaken in an anaerobic chamber (Plas-Lab Inc. 855 Series, Lansing, MI, USA). Pd catalyst and high purity H_2/N_2 mixing gases (5%/95%) were used to keep anaerobic conditions (<0.1 ppm O_2) at 25°C.

1.2. Preparation of uncoated and CMC-coated Pd-nZVI particles

All steps in the synthesis of the CMC-coated and uncoated Pd-nZVI particles were performed in an anaerobic chamber in order to minimize the possibility of nZVI oxidation. The synthesis method for the non-coated particles was in accordance with our previous work (He et al., 2016), and the pre-synthesis steps were adopted for the synthesis of CMC-coated particles (He and Zhao, 2007). In comparison to the synthetic method for the uncoated particles, the Fe(II) solution was mixed with the CMC solution for at least half an hour to allow for the formation of an Fe(II)-CMC complex prior to the addition of borohydride to form Fe(0). Impregnation of Pd onto the surface of Fe(0) was then undertaken using a procedure identical to that for the non-stabilized particles.

The CMC-stabilized Pd-nZVI particles were then rinsed with the exception that only de-aerated Milli-Q water was employed for rinsing (i.e. the rinsing step with methanol was not employed) and the oven temperature was maintained at 40°C or just below.

1.3. Particle characterization

A Phillips CM200 transmission electron microscope (TEM) was used to examine the morphology, structure and the particle size distribution (PSD) of the prepared particles. Elemental analysis of the nanoparticles was obtained by energy-dispersive X-ray spectroscopy (EDX). Further details of TEM and EDX analysis have been shown in our previous study (Ma et al., 2016). The Pd content of the particles and extent of Fe and Pd released through the course of PCB degradation were quantified by ICP-MS analysis of acid digested samples and acidified filtered solutions respectively. The specific surface area (SSA) of the particles was determined using the Brunauer–Emmett–Teller (BET) gas adsorption method (Micrometrics, Tristar 3000). Further insight into the particle size of the nZVI assemblages was obtained by sedimentation experiments undertaken inside the anaerobic chamber by monitoring the absorbance of the suspensions at a wavelength of 508 nm as a function of time in both FW and SW environments (Phenrat et al., 2007).

1.4. PCB degradation experiments

Gas chromatography (GC) analysis was applied for measuring the degradation of PCB with the detailed methods as reported in our previous work (He et al., 2016). The concentrations of PCB and its major product, biphenyl, were determined by injecting 1 μL of the extracted organic sample into a GC (HP-7890) equipped with ECD and FID detectors for analysis, respectively, of the parent PCB compound and biphenyl. The temperature programs and other parameters (such as gas flow rate) were set up and modified according to previous publication (Lowry and Johnson, 2004). The quantification of each analyte was undertaken by converting the GC readings into concentrations using a five-point calibration curve ($R^2 > 0.98$). The extent of Fe and Pd dissolution during the reaction was monitored using ICP-OES (He et al., 2016). The kinetic modeling software (KinTek Explorer), which employed the Bulirsch–Stoer algorithm for numerical integration to derive the time course of various chemical reactions a given reaction scheme (Johnson et al., 2009). Nonlinear regression was then used to fit data based on the Levenberg–Marquardt method to examine the goodness of fit of the proposed reaction schemes to the Fe dissolution data (Johnson et al., 2009). More details on Fe dissolution kinetic model can be found in our previous work (He et al., 2016).

2. Results and discussion

2.1. Characterization

TEM images of non-stabilized and CMC-stabilized Pd-nZVI nanoparticles (before reaction) are provided in Fig. 1. The non-

stabilized particles are spherical with an average diameter of 143.2 nm though with a quite broad distribution (±97.4 nm). They exhibit a distinct chain-like structure with Fe(0) assemblages apparently coated by an oxide shell (Appendix A Fig. S1a). The stabilized particles also exhibit a chain-like structure though the average size of the individual particles are substantially smaller than that of the non-stabilized particles (at 47.1 ± 14.7 nm) and exhibit a much narrower size distribution. The results of BET analyses indicate a specific surface area of 7.32 and 15.2 m^2/g for the non-stabilized and stabilized particles, respectively. The EDX pattern of both particles shows the presence of Fe and Pd (Appendix A Fig. S1b) indicating that Pd was successfully loaded on both particle types. Sedimentation experiments were undertaken to further investigate the stability of the CMC-coated particles in both FW and SW (Appendix A Fig. S2). Both particles exhibit rapid initial settling, however, sedimentation rate of the CMC-coated particles decreases to some extent after 10 min of exposure to both FW and SW whilst the uncoated particles continue to settle. As such, CMC has been shown to be an effective nZVI stabilizer, resulting in the production of particles with a narrower particle size distribution and relatively slower sedimentation rate in FW compared to the non-stabilized particles. Nevertheless, the results of SW sedimentation experiments indicate that the effectiveness of CMC stabilization is limited under high salinity conditions. In terms of the effect of different water matrices on the particle reactivity, the removal of PCB in SW is not significantly different to that in FW. On closer inspection of the degradation process, however, it is apparent that the dechlorinated product (i.e. biphenyl) is produced more slowly and to a lesser degree in SW than that in FW (Appendix A Fig. S3a). A similar trend was observed in the case of PCB degradation by CMC-coated Pd-nZVI, with lesser extent of PCB removal and biphenyl formation compared to bare Pd-nZVI (Appendix A Fig. S3b).

2.2. Effect of EDTA on PCB degradation by non-stabilized Pd-nZVI

The effect of EDTA on PCB dechlorination and biphenyl production by non-stabilized Pd-nZVI is shown in Fig. 2 and Appendix A Fig. S4, respectively. The significant increase in PCB reduction following the addition of EDTA observed here is similar to that observed in previous studies for other target contaminants, and is ascribed to EDTA-mediated dissolution of the iron oxide passivating layer (Zhou et al., 2008; Zhang et al., 2011). The depassivation process is initiated by the adsorption of EDTA to the Fe oxide surface, followed by dissociation of the complex with subsequent release of Fe(II)- and/or Fe(III)-EDTA to solution (Nowack and Sigg, 1997; He et al., 2016). The resultant decrease or even removal of the outer iron oxides shell appears to restore the electron transfer abilities of nZVI, presumably by reexposing the Fe(0) core and Pd islets, leading to the recovery of the reactivity of these Pd/nZVI assemblages (He et al., 2016).

To further verify this hypothesis, the simultaneous dissolution of Fe and Pd during reaction with EDTA was monitored with the results displayed in Fig. 3. The bulk solution underwent a remarkable increase in the release of dissolved
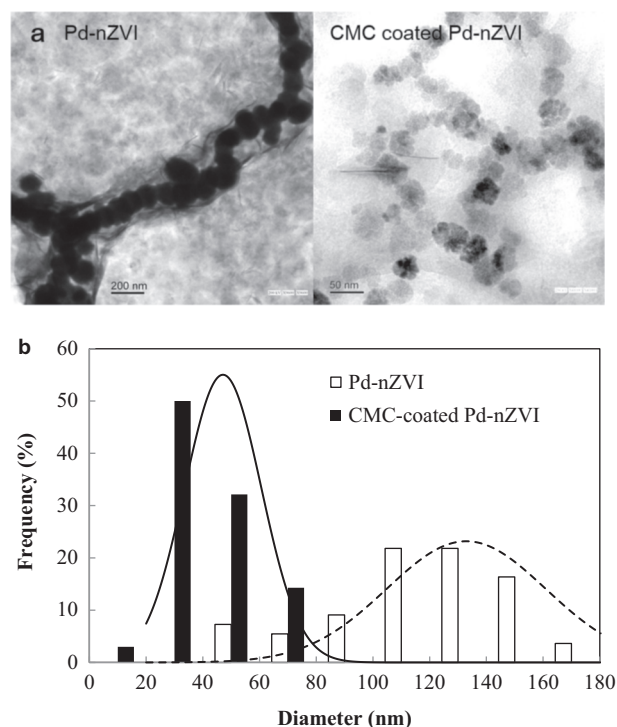

Fig. 1 – TEM images of non-stabilized (left) and CMC-stabilized (right) Pd doped nanoscale zero valent iron (Pd-nZVI) particles and particle size distributions of both particles (b).

Fe following the addition of EDTA, whereas a negligible concentration of dissolved Fe was detected throughout the reaction period in the absence of EDTA. This sharp increase in the release of dissolved iron following the addition of EDTA agrees with our hypothesis that EDTA induces dissolution of the passivating oxide layer. It is also noted that there is no significant release of Pd from Pd-nZVI particles in the presence of EDTA, which is expected if there is less oxidized
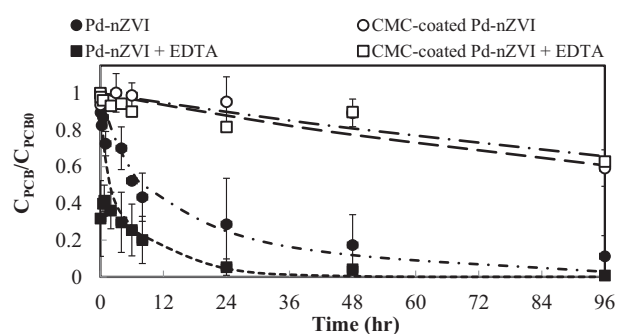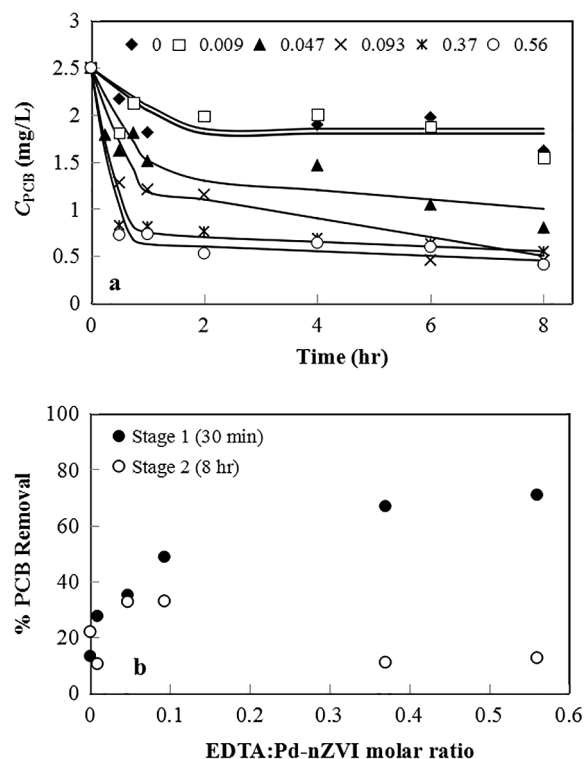

Fig. 2 – Degradation of PCB by CMC-stabilized and non-stabilized Pd-nZVI in the absence or presence of EDTA (•: Pd-nZVI; ○: CMC-Coated Pd-nZVI; ■: Pd-nZVI+EDTA; □: CMC-coated Pd-nZVI+EDTA). Error bars are standard deviations from triplicate measurements. Experimental conditions: C_{PCB0}=2.5 mg/L; $C_{Pd-nZVI0}$=6 g/L; C_{EDTA}=100 mmol/L.
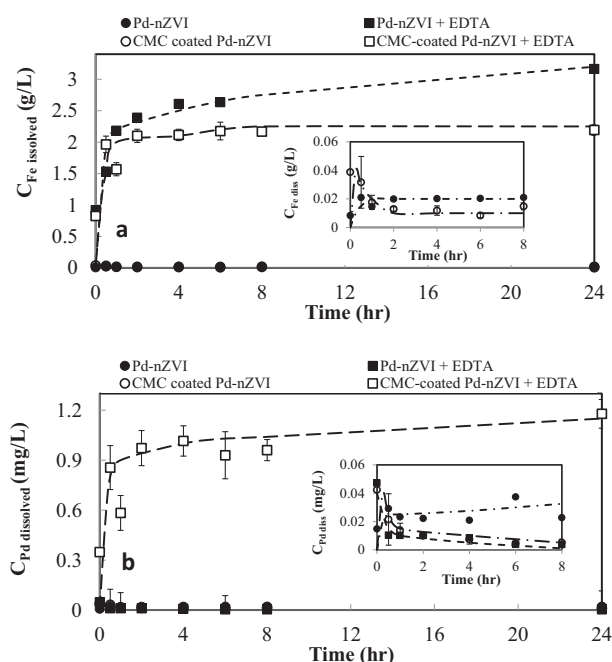
Fig. 3 – Comparison of dissolved Fe concentration (a) and dissolved Pd concentration (b) following the addition of EDTA (•: Pd-nZVI; ○: CMC-Coated Pd-nZVI; ■: Pd-nZVI+EDTA; □: CMC-coated Pd-nZVI+EDTA). Error bars are standard deviations from triplicate measurements. Experimental conditions: C_{PCB0}=2.5 mg/L; $C_{Pd-nZVI0}$= 6 g/L; C_{EDTA0}=100 mmol/L.

Fig. 4 – (a) PCB degradation by non-stabilized Pd-nZVI particles in the presence of different molar proportions of EDTA and Pd-nZVI. Straight lines represent linear fits to the degradation of the "slow phase" (i.e. after 30 mins, taken as the starting point of the slow phase); (b) the amount of PCB dechlorinated during the first 30 mins (Stage 1) or from 0.5 to 8 hr (Stage 2) in the presence of various EDTA loadings. Experimental conditions: C_{PCB0} = 2.5 mg/L; $C_{Pd-nZVI0}$ = 6 g/L.

Pd present. As such, we can conclude that the major role of EDTA is to dissolve the passivation film surrounding the Fe(0) core.

As can be seen in Fig. 4a, PCB degradation was typically quite rapid initially (Stage 1: 0–0.5 hr) but slowed to varying degrees (Stage 2: 0.5–8 hr) as the reaction proceeded, despite the presence of EDTA. Analysis of the degradation data over the first 30 min (Fig. 4b) enabled determination of the initial rapid degradation rate with a steady increase in the initial rate of PCB degradation observed on increasing the molar ratio of EDTA to nZVI from 0 to 0.56 (corresponding to an EDTA concentration of 60 mmol/L and an nZVI concentration of 107.1 mmol/L). Based on the results obtained, it would seem reasonable to conclude that, for the first stage, the addition of EDTA results in the removal of the original Fe oxide layer formed due to the anaerobic passivation by water and/or other solvents during the synthesis process, leading to a rapid recovery in the availability of reactive Fe(0) sites for decontamination. The rapid initial increase in the rates of Fe dissolution and PCB degradation (Figs. 4 and 5) observed with increasing EDTA loadings supports our hypothesis that a higher concentration of EDTA is more favorable for removal of the original Fe passivation layer, resulting in an initial rapid rate of PCB dechlorination. Following the elimination of the original oxide layer, fresh Fe oxide layers can be continually generated due to the exposure of the Fe(0) core to water and/or other matrix components accompanying PCB decomposition. The growing Fe oxide passivation layer will decrease the

accessibility of Fe(0) and Pd islets resulting in a reduction in the number of sites available for reductive dechlorination and, thus, a reduction in the rate of PCB dechlorination. This is consistent with our observation that PCB degradation significantly decreased after (approximately) 30 min (Fig. 4). As such, EDTA, if present at sufficient concentrations, will inhibit the formation of *in situ* generated Fe oxide layers by continually removing these layers and, consequently, will ensure that the high reactivity of the Pd-nZVI particles is maintained (Appendix A Fig. S5). However, it is difficult to observe a clear trend with varying concentration of EDTA at Stage 2 (0.5–8 hr) from Fig. 4b, presumably due to the complex nature of reactions occurring simultaneously. These reactions would include the formation of *in situ* generated passivation layers and their subsequent removal by EDTA, variability in the accessibility of Pd islets, ligand-induced nZVI dissolution and particle sedimentation due to magnetic attraction following complete removal of the Fe oxide layer in the presence of excessive EDTA (Appendix A Fig. S6). These potential factors will solely or interactively affect the efficiency of electron transfer in either a positive or negative manner, complicating PCB dechlorination. It should be noted that, in the case of high dosages of EDTA, a dramatic decrease in the concentration of reactants (i.e. PCB) following the first 30 min may also
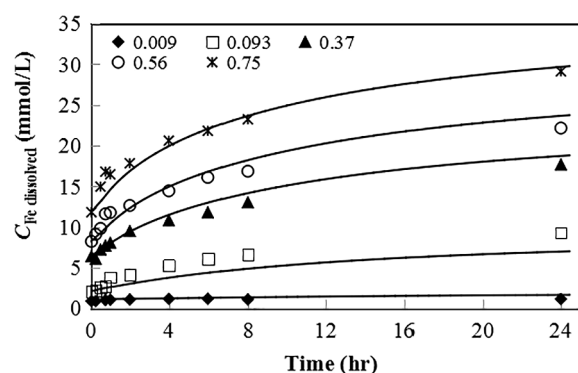
Fig. 5 – Dissolution of Fe from non-stabilized Pd-nZVI at various molar ratios of EDTA to Pd-nZVI. Symbols are experimental data; lines are model values. Experimental conditions: $C_{Pd-nZVI0}$ = 6.0 g/L.

contribute to the rapid reduction in the rate of PCB dechlorination.

Despite the fact that EDTA can effectively eliminate the formation of an Fe oxide passivating film, excessive removal of Fe oxide layers by EDTA may lead to a significant loss of Fe (0) (through dissolution), reducing the concentration of the Pd-nZVI assemblage available for ongoing contaminant degradation. It can be observed from Fig. 5 that, following 24 hr of reaction, the percentage of Fe released into solution increased dramatically from 8.7% to 27.2% with an increase in the molar ratio of EDTA to nZVI from 0.093 (i.e. 10 mmol/L) to 0.75 (i.e. 80 mmol/L). Our recently developed mechanistic-based kinetic model for ligand-promoted dissolution of Pd-nZVI is able to satisfactorily describe the time variation in dissolved Fe(II) concentrations released from the interactions of Pd-nZVI with SW in the presence of various concentrations of EDTA (Appendix A Table S1). This model consists of three main sections: (1) anaerobic passivation of nZVI (Reactions 1–3 in Appendix A Table S1); (2) dissolution of Fe oxide layers induced by EDTA (Reactions 4–6 in Appendix A Table S1); (3) complexation reactions between EDTA and other divalent cations present in the reaction medium (mainly Ca(II) and Mg(II) in this study) (Reaction 7–8 in Appendix A Table S1) and (4) complexation reactions between EDTA and Ca(II)/Mg(II). Further details on this Fe dissolution kinetic model, including the calculation of stability and formation rate constants for metal-EDTA complexes and constrains of fitting parameters, are provided in our previous work (He et al., 2016).

The dissolution of such a high percentage of Fe is neither beneficial nor economically sensible for contaminant reduction and provides an explanation for the lack of any further enhancement in reactivity when excess EDTA (i.e. molar ratios of EDTA to nZVI > 0.093) is employed. In addition to this, increasing the EDTA concentration increased the rate of particle sedimentation, most likely due to enhanced magnetic attraction, and therefore aggregation, of the depassivated nZVI particles (as demonstrated in Appendix A Fig. S6). Particle aggregation decreases the availability of nZVI reactive surface sites, including Pd, collectively resulting in a reduction in degradation efficiency (Appendix A Fig. S7). In summary,

despite the depassivation capability of EDTA demonstrated in this study, the dosage serves a crucial factor for optimizing PCB dechlorination. A moderate dosage can lead to increased reactivity of the Pd-nZVI assemblages, whereas inappropriately high dosages of EDTA will lead to either an accumulation of an Fe oxide layer or rapid consumption of nZVI through ligand-promoted particle dissolution. As such, there is an empirical optimum EDTA to Pd-nZVI molar ratio, determined here to be 0.1, for the depassivation of non-stabilized Pd-nZVI particles in SW.

2.3. Effect of EDTA on PCB degradation by CMC-coated Pd-nZVI

It is well-known that stabilizers are capable of preventing particle aggregation via electrostatic or steric repulsion forces, thereby increasing the surface area available for contaminant degradation as well as enhancing the mobility of the colloidal particles (Hunter, 2001). Many studies have demonstrated the positive effect of stabilizers towards nZVI-induced degradation of various chlorinated compounds (He et al., 2006; He and Zhao, 2008; Zhan et al., 2008; Sakulchaicharoen et al., 2010). In this study we found, perhaps surprisingly, that CMC addition actually impeded contaminant degradation. Fig. 2 demonstrates that ~30% of the PCB initially present was removed after four days of exposure to CMC-stabilized Pd-nZVI, compared to ~90% of PCB removal using non-stabilized particles. The high loss in reactivity of CMC-stabilized Pd-nZVI relative to that of non-stabilized Pd-nZVI cannot be explained by an increase in particle aggregation as a slight decrease in the sedimentation rate of the CMC-stabilized Pd-nZVI in SW was observed (Appendix A Fig. S2). In addition to this, the CMC-stabilized particles possessd a smaller average particle size relative to the non-stabilized Pd-nZVI particles (Fig. 1). As the reactivity of bimetallic particles depends strongly on the loading and speciation of the doped metal present, any change in the loading and speciation of Pd on the nZVI particle surface will result in a significant change in the reactivity of CMC-stabilized Pd-nZVI towards PCB degradation. Indeed, according to the results of our ICP analyses, our attempts to prepare Pd loaded particles using CMC-coated nZVI particles resulted in a decrease in Pd loading (0.198 mg or 0.66% (W/W) of Fe) when compared to the uncoated particles (0.291 mg or 0.97% (W/W) of Fe), despite using the same concentration of Pd for the synthesis of both particle types. To further investigate and verify this effect, different Pd loadings were employed for nZVI-mediated PCB degradation. The results (Appendix A Fig. S8) demonstrate that, with increasing Pd loading, the decomposition of PCB does increase as expected. In particular the reaction was significantly accelerated on increasing the Pd loading from 0.5% to 1%, though further enhancement was not particularly evident when the Pd loading was increased from 2% to 3%.

Whilst EDTA is able to significantly improve the reactivity of non-stabilized Pd-nZVI, the combined effect of ligand and stabilizer on particle reactivity has not as yet been reported. As such, the effect of EDTA towards PCB degradation by CMC-coated palladized particles was evaluated under the same conditions as described above. As is clearly evident from the results shown in Fig. 2, the addition of EDTA was not able to

provide any significant improvement in the degradation of PCB when employing CMC-stabilized particles. This is despite the removal of Fe passivating layers being observed following the addition of EDTA (Fig. 3a). Meanwhile, as shown in Fig. 3b, following the addition of EDTA, the dissolution of Pd from the CMC-coated particles was significantly higher than was the case for the non-coated particles. Considering that EDTA is only capable of forming a complex with oxidized Pd species, this observation indicates that the CMC coating partially impedes the reduction of Pd(II) to Pd(0) during particle synthesis. This is presumed to be due to the inhibited contact between Fe(0) and Pd particles, and the Pd salts instead chelating with functional groups on CMC. It should be noted that although there was only ~3% of total loaded Pd released into the aqueous phase following the addition of 100 mmol/L EDTA (Fig. 3b) in the case of CMC-stabilized nZVI, the actual amount of oxidized Pd is likely to be underestimated as much of the EDTA will be coordinated with Fe(II) and Fe(III) resulting in less EDTA being available for complexation with oxidized Pd species. Therefore, the possible explanations for the lack of any improvement in reactivity during the EDTA mediated depassivation process are that (1) doped Pd(II) could be removed following the addition of EDTA and/or (2) Pd(0) does not dominate Pd speciation, leading to a lower efficiency in the transformation of H_2 to atomic H.

To summarize, compared to the results with non-CMC coated particles, a lower amount of total Pd and the presence of oxidized Pd species on the CMC-coated particles result in a much lower amount of reactive Pd(0) being available on the CMC-coated particles relative to the uncoated particles for the production of atomic hydrogen and the reduction of contaminants. In the schematic presented in the Supplementary Material (Appendix A Fig. S9), it is demonstrated how the presence of CMC can also impede the deposition of Pd(II) onto the surface of nZVI, which is required for the reduction of Pd(II) to Pd(0). Instead, Pd(II) is retained within the CMC branches, with the addition of EDTA resulting in complexation with Pd(II) and the release of Pd(II)-EDTA into solution. As such, the use of CMC-coated particles prepared in the manner described in this study, with or without the use of a depassivating agent such as EDTA, is not recommended for use in a SW environment.

3. Conclusion

While bimetallic Pd-nZVI particles are recognized to be effective for degrading persistent organic compounds such as PCBs, very little attention has been given to the efficacy of these particles in SW environments where such contaminants are likely to be found. We have shown here that Pd-nZVI assemblages are capable of dechlorinating PCB though degradation, but this reactivity soon ceases and is attributed to rapid passivation of the nZVI surface due to the formation of a coating of iron oxides. The addition of EDTA is capable of accelerating PCB dechlorination via eliminating these passivating layers however an appropriate dosage of EDTA needs to be employed. Too little EDTA is unable to eliminate early onset passivation whilst too much leads to excessive loss of

iron to solution. In this study, an optimum molar ratio of EDTA to nZVI of 0.1 was identified. A conceptual kinetic model was developed to describe the complex interactions occurring in the nZVI/water/Fe oxyhydroxide/Ca(II)/Mg(II)/EDTA system over a range of EDTA concentrations in SW, with this model of great value in describing the possible depassivation mechanisms occurring in SW environments. It should be noted that the application of EDTA for depassivation would introduce another environmental hazard; therefore, a more environmental-friendly complexing agent with comparable coordination abilities to EDTA should be investigated in the future. For example, ethylenediamine-N,N′-disuccinic acid, a biodegradable chelating agent with the similar chelating abilities to EDTA is a possible alternative complexing/depassivating agent (Tandy et al., 2003).

Whilst it has been shown that the application of CMC failed to enhance the reactivity of Pd-nZVI particles in SW, steric stabilizers such as PVP may provide a viable alternative in such environments. This is on the proviso that, as occurred with CMC in this study, the stabilizer does not affect the contact between Pd(II) and the surface of nZVI particles during bimetallic particle synthesis, inhibiting the reduction of Pd(II) to Pd(0) and therefore reducing the uptake of reactive Pd(0) onto the particle surface.

Appendix A. Supplementary data

Supplementary data to this article can be found online at https://doi.org/10.1016/j.jes.2018.09.002.

REFERENCES

Alqadami, A.A., Naushad, M., Alothman, Z.A., Ghfar, A.A., 2017. Novel metal–organic framework (MOF) based composite material for the sequestration of U(VI) and Th(IV) metal ions from aqueous environment. ACS Appl. Mater. Interfaces 9, 36026–36037.

Alqadami, A.A., Naushad, M., Alothman, Z.A., Ahamad, T., 2018. Adsorptive performance of MOF nanocomposite for methylene blue and malachite green dyes: Kinetics, isotherm and mechanism. J. Environ. Manag. 223, 29–36.

Bergen, B.J., Nelson, W.G., Pruell, R.J., 1996. Comparison of nonplanar and coplanar PCB congener partitioning in seawater and bioaccumulation in blue mussels (*Mytilus edulis*). Environ. Toxicol. Chem. 15, 1517–1523.

Coutts, J.L., Devor, R.W., Aitken, B., Hampton, M.D., Quinn, J.W., Clausen, C.A., et al., 2011. The use of mechanical alloying for the preparation of palladized magnesium bimetallic particles for the remediation of PCBs. J. Hazard. Mater. 192, 1380–1387.

Danis, B., Cotret, O., Teyssié, J.L., Fowler, S.W., Warnau, M., 2004. Coplanar PCB 77 uptake kinetics in the sea star *Asterias rubens* and subsequent effects on reactive oxygen species (ROS) production and levels of cytochrome P450 immunopositive proteins (CYP1A-IPP). Mar. Ecol. Prog. Ser. 279, 117–128.

Elliott, D.W., Zhang, W., 2001. Field assessment of nanoscale bimetallic particles for groundwater treatment. Environ. Sci. Technol. 35, 4922–4926.

Geiger, C.L., Carvalho-Knighton, K., Novaes-Card, S., Maloney, P., Devor, R., 2009. Chapter 1 Environmental applications of nanoscale and microscale reactive metal particles. ACS Symposium Series ebook, February 1, 2010, pp. 1–20 https://doi.org/10.1021/bk-2009-1027.ch001.

Ghosh, U., Zimmerman, J.R., Luthy, R.G., 2003. PCB and PAH speciation among particle types in contaminated harbor sediments and effects on PAH bioavailability. Environ. Sci. Technol. 37, 2209–2217.

Grieger, K.D., Fjordbøge, A., Hartmann, N.B., Eriksson, E., Bjerg, P. L., Baun, A., 2010. Environmental benefits and risks of zerovalent iron nanoparticles (nZVI) for in situ remediation: Risk mitigation or trade-off? J. Contam. Hydrol. 118, 165–183.

He, F., Zhao, D., 2007. Manipulating the size and dispersibility of zerovalent iron nanoparticles by use of carboxymethyl cellulose stabilizers. Environ. Sci. Technol. 41, 6216–6221.

He, F., Zhao, D., 2008. Hydrodechlorination of trichloroethene using stabilized Fe-Pd nanoparticles: Reaction mechanism and effects of stabilizers, catalysts and reaction conditions. Appl. Catal. B-Environ. 84, 533–540.

He, F., Zhao, D., Liu, J., Roberts, C.B., 2006. Stabilization of Fe–Pd nanoparticles with sodium carboxymethyl cellulose for enhanced transport and dechlorination of trichloroethylene in soil and groundwater. Ind. Eng. Chem. Res. 46, 29–34.

He, D., Ma, X., Jones, A.M., Ho, L., Waite, T.D., 2016. Mechanistic and kinetic insights into the ligand-promoted depassivation of bimetallic zero-valent iron nanoparticles. Environ. Sci. Nano 3, 737–744.

Hunter, R.J., 2001. Foundations of Colloid Science. 2nd ed. Oxford University Press, Oxford, UK.

Johnson, K.A., Simpson, Z.B., Blom, T., 2009. Global kinetic explorer: a new computer program for dynamic simulation and fitting of kinetic data. Anal. Biochem. 387, 20–29.

Kim, J.S., Shea, P.J., Yang, J.E., Kim, J., 2007. Halide salts accelerate degradation of high explosives by zerovalent iron. Environ. Pollut. 147, 634–641.

Li, L., Fan, M., Brown, R.C., Van Leeuwen, J., Wang, J., Wang, W., et al., 2006. Synthesis, properties, and environmental applications of nanoscale iron-based materials: a review. Crit. Rev. Environ. Sci. Technol. 36, 405–431.

Liang, L.P., Sun, W., Guan, X.H., Huang, Y.Y., Choi, W.Y., Bao, H.L., et al., 2014. Weak magnetic field significantly enhances selenite removal kinetics by zero valent iron. Water Res. 49, 371–380.

Lien, H., Zhang, W., 2001. Nanoscale iron particles for complete reduction of chlorinated ethenes. Colloid Surface A 191, 97–105.

Lien, H., Zhang, W., 2007. Nanoscale Pd/Fe bimetallic particles: catalytic effects of palladium on hydrodechlorination. Appl. Catal. B-Environ. 77, 110–116.

Liou, Y.H., Lo, S., Kuan, W.H., Lin, C., Weng, S.C., 2006. Effect of precursor concentration on the characteristics of nanoscale zerovalent iron and its reactivity of nitrate. Water Res. 40, 2485–2492.

Liu, Y., Lowry, G.V., 2006. Effect of Particle Age (Fe0 Content) and Solution pH on nZVI reactivity: H2 evolution and TCE dechlorination. Environ. Sci. Technol. 40, 6085–6090.

Lowry, G.V., Johnson, K.M., 2004. Congener-specific dechlorination of dissolved PCBs by microscale and nanoscale zerovalent iron in a water/methanol solution. Environ. Sci. Technol. 38, 5208–5216.

Ma, X., He, D., Jones, A.M., Collins, R.N., Waite, T.D., 2016. Reductive reactivity of borohydride- and dithionite-synthesized iron-based nanoparticles: a comparative study. J. Hazard. Mater. 303, 101–110.

Mayes, B.A., McConnell, E.E., Neal, B.H., Brunner, M.J., Hamilton, S. B., Sullivan, T.M., et al., 1998. Comparative carcinogenicity in Sprague–Dawley rats of the polychlorinated biphenyl mixtures Aroclors 1016, 1242, 1254, and 1260. Toxicol. Sci. 41, 62–76.

Mikszewski, A., 2004. Emerging technologies for the in situ remediation of PCB-contaminated soils and sediments: bioremediation and nanoscale zero-valent iron. US EPA Environmental Innovation Program Report, Washington DC, USA.

Nowack, B., Sigg, L., 1997. Dissolution of Fe(III) (hydr)oxides by metal-EDTA complexes. Geochim. Cosmochim. Acta 61, 951–963.

O'Carroll, D., Sleep, B., Krol, M., Boparai, H., Kocur, C., 2013. Nanoscale zero valent iron and bimetallic particles for contaminated site remediation. Adv. Water Resour. 51, 104–122.

Phenrat, T., Saleh, N., Sirk, K., Tilton, R., Lowry, G., 2007. Aggregation and sedimentation of aqueous nanoscale zerovalent iron dispersions. Environ. Sci. Technol. 41, 284–290.

Ponder, S.M., Darab, J.G., Mallouk, T.E., 2000. Remediation of Cr(VI) and Pb(II) aqueous solutions using supported nanoscale zerovalent iron. Environ. Sci. Technol. 34, 2564–2569.

Qin, H.J., Li, J.X., Yang, H.Y., Pan, B.C., Zhang, W.M., Guan, X.H., 2017. Coupled effect of ferrous ion and oxygen on the electron selectivity of zerovalent iron for selenate sequestration. Environ. Sci. Technol. 51, 5090–5097.

Ramos, M.A.V., Yan, W., Li, X., Koel, B.E., Zhang, W., 2009. Simultaneous oxidation and reduction of arsenic by zerovalent Iron nanoparticles: understanding the significance of the core–shell structure. J. Phys. Chem. C 113, 14591–14594.

Reinsch, B.C., Forsberg, B., Penn, R.L., Kim, C.S., Lowry, G.V., 2010. Chemical transformations during aging of zerovalent iron nanoparticles in the presence of common groundwater dissolved constituents. Environ. Sci. Technol. 44, 3455–3461.

Sakulchaicharoen, N., O'Carroll, D.M., Herrera, J.E., 2010. Enhanced stability and dechlorination activity of pre-synthesis stabilized nanoscale FePd particles. J. Contam. Hydrol. 118, 117–127.

Schrick, B., Blough, J.L., Jones, A.D., Mallouk, T.E., 2002. Hydrodechlorination of trichloroethylene to hydrocarbons using bimetallic nickel–iron nanoparticles. Chem. Mater. 14, 5140–5147.

Shih, Y., Chen, Y., Chen, M., Tai, Y., Tso, C., 2009. Dechlorination of hexachlorobenzene by using nanoscale Fe and nanoscale Pd/Fe bimetallic particles. Colloid Surf. A 332, 84–89.

Song, H., Carraway, E.R., 2006. Reduction of chlorinated methanes by nano-sized zero-valent iron. Kinetics, pathways, and effect of reaction conditions. Environ. Eng. Sci. 23, 272–284.

Sun, Y.K., Guan, X.H., Wang, J.M., Meng, X.G., Xu, C.H., Zhou, G.M., 2014. Effect of weak magnetic field on arsenate and arsenite removal from water by zerovalent iron: an XAFS investigation. Environ. Sci. Technol. 48, 6850–6858.

Tandy, S., Bossart, K., Mueller, R., Ritschel, J., Hauser, L., Schulin, R., et al., 2003. Extraction of heavy metals from soils using biodegradable chelating agents. Environ. Sci. Technol. 38, 937–944.

Tee, Y., Grulke, E., Bhattacharyya, D., 2005. Role of Ni/Fe nanoparticle composition on the degradation of trichloroethylene from water. Ind. Eng. Chem. Res. 44, 7062–7070.

US EPA, 2008. Nanotechnology for site remediation fact sheet. U.S. Environmental Protection Agency, Washington, DC.

Wang, C., Zhang, W., 1997. Synthesizing nanoscale iron particles for rapid and complete dechlorination of TCE and PCBs. Environ. Sci. Technol. 31, 2154–2156.

Wei, J., Xu, X., Liu, Y., Wang, D., 2006. Catalytic hydrodechlorination of 2,4-dichlorophenol over nanoscale Pd/Fe: reaction pathway and some experimental parameters. Water Res. 40, 348–354.

Wei, Y., Wu, S., Chou, C., Che, C., Tsai, S., Lien, H., 2010. Influence of nanoscale zero-valent iron on geochemical properties of groundwater and vinyl chloride degradation: a field case study. Water Res. 44, 131–140.

WHO, 2010. Exposure to Dioxins and Dioxin-Like Substances: A Major Public Health Concern. World Health Organization, Geneva.

Xie, Y., Cwiertny, D.M., 2010. Use of dithionite to extend the reactive lifetime of nanoscale zero-valent iron treatment systems. Environ. Sci. Technol. 44, 8649–8655.

Xie, Y.Y., Fang, Z.Q., Qiu, X.H., Tsang, E.P., Liang, B., 2014. Comparisons of the reactivity, reusability and stability of four different zero-valent iron-based nanoparticles. Chemosphere 108, 433–436.

Xie, Y.H., Yi, Y., Qin, Y.H., Wang, L.T., Liu, G.M., Wu, Y.L., et al., 2016. Perchlorate degradation in aqueous solution using chitosan-stabilized zero-valent iron nanoparticles. Sep. Purif. Technol. 171, 164–173.

Xin, J., Tang, F.L., Zheng, X.L., Shao, H.B., Kolditz, O., Lu, X., 2016. Distinct kinetics and mechanisms of mZVI particles aging in saline and fresh groundwater: H_2 evolution and surface passivation. Water Res. 100, 80–87.

Xu, J., Bhattacharyya, D., 2006. Fe/Pd nanoparticle immobilization in microfiltration membrane pores: Synthesis, characterization, and application in the dechlorination of polychlorinated biphenyls. Ind. Eng. Chem. Res. 46, 2348–2359.

Yan, S., Hua, B., Bao, Z., Yang, J., Liu, C., Deng, B., 2010a. Uranium (VI) removal by nanoscale zerovalent iron in anoxic batch systems. Environ. Sci. Technol. 44, 7783–7789.

Yan, W., Herzing, A.A., Li, X., Kiely, C.J., Zhang, W., 2010b. Structural evolution of Pd-doped nanoscale zero-valent iron (nZVI) in aqueous media and implications for particle aging and reactivity. Environ. Sci. Technol. 44, 4288–4294.

Yang, G.C.C., Lee, H., 2005. Chemical reduction of nitrate by nanosized iron: kinetics and pathways. Water Res. 39, 884–894.

Yin, W., Wu, J., Li, P., Wang, X., Zhu, N., Wu, P., et al., 2012. Experimental study of zero-valent iron induced nitrobenzene reduction in groundwater: the effects of pH, iron dosage, oxygen and common dissolved anions. Chem. Eng. J. 184, 198–204.

Zhan, J., Zheng, T., Piringer, G., Day, C., McPherson, G.L., Lu, Y., Papadopoulos, K., et al., 2008. Transport characteristics of nanoscale functional zerovalent iron/silica composites for in situ remediation of trichloroethylene. Environ. Sci. Technol. 42, 8871–8876.

Zhang, W., Wang, C., Lien, H., 1998. Treatment of chlorinated organic contaminants with nanoscale bimetallic particles. Catal. Today 40, 387–395.

Zhang, X., Deng, B., Guo, J., Wang, Y., Lan, Y., 2011. Ligand-assisted degradation of carbon tetrachloride by microscale zero-valent iron. J. Environ. Manag. 92, 1328–1333.

Zhou, H., He, Y., Lan, Y., Mao, J., Chen, S., 2008. Influence of complex reagents on removal of chromium(VI) by zero-valent iron. Chemosphere 72, 870–874.

Zhu, B., Lim, T., 2007. Catalytic reduction of chlorobenzenes with Pd/Fe nanoparticles: reactive sites, catalyst stability, particle aging, and regeneration. Environ. Sci. Technol. 41, 7523–7529.